Inhibition of cAMP-Dependent Protein Kinase under Conditions Occurring in the Cardiac Dyad during a Ca^{2+} Transient

Peter P. Jones,*† Hojjat Bazzazi,†‡ Gary J. Kargacin,† and John Colyer*
*Institute of Membrane and Systems Biology, University of Leeds, Leeds LS2 9JT, United Kingdom; †Department of Physiology and Biophysics, University of Calgary, Calgary, Alberta T2N 4N1, Canada; and ‡Department of Biomedical Engineering, The Johns Hopkins University, Baltimore, Maryland 21205

ABSTRACT The space between the t-tubule invagination and the sarcoplasmic reticulum (SR) membrane, the dyad, in ventricular myocytes has been predicted to experience very high [Ca^{2+}] for short periods of time during a Ca^{2+} transient. The dyadic space accommodates many protein kinases responsible for the regulation of Ca^{2+} handling proteins of the cell. We show in vitro that cAMP-dependent protein kinase (PKA) is inhibited by high [Ca^{2+}] through a shift in the ratio of CaATP/MgATP toward CaATP. We further generate a three-dimensional mathematical model of Ca^{2+} and ATP diffusion within dyad. We use this model to predict the extent to which PKA would be inhibited by an increased CaATP/MgATP ratio during a Ca^{2+} transient in the dyad in vivo. Our results suggest that under normal physiological conditions a myocyte paced at 1 Hz would experience up to 55% inhibition of PKA within the cardiac dyad, with inhibition averaging 5% throughout the transient, an effect which becomes more pronounced as the myocyte contractile frequency increases (at 7 Hz, PKA inhibition averages 28% across the dyad throughout the duration of a Ca^{2+} transient).

INTRODUCTION

The calcium concentration ([Ca^{2+}]) in cardiac myocytes varies significantly both spatially and temporally during a contraction. Cytosolic-free calcium ([Ca^{2+}]$_{free}$) typically averages ~150 nM at rest but increases to ~1 μM during a contraction, with half-maximal contraction occurring at ~600 nM (1). Subsequent relaxation occurs when [Ca^{2+}]$_{free}$ falls to ~200 nM (2). In organelles within the myocyte such as the sarcoplasmic reticulum (SR), the [Ca^{2+}] is much more difficult to measure accurately. Shannon and Bers (3) have estimated the total SR [Ca^{2+}] in quiescent myocytes to be as high as 14 mM although the free [Ca^{2+}] in the SR lumen is likely to be lower than this.

During contraction, Ca^{2+} enters the myocyte through the voltage-gated L-type calcium channels (dihydropyridine receptors, DHPR) in the t-tubular invagination of the sarcolemma. This triggers an additional, greater release of Ca^{2+} from the SR through the ryanodine receptors (RYR), a process termed calcium-induced calcium release (CICR, (4)). The cell architecture is such that both Ca^{2+} entry into the cell and Ca^{2+} release from the SR deposit Ca^{2+} into the cardiac dyad, the physical space formed between the t-tubule and the opposing SR membrane. The dyadic cleft between the t-tubule and SR membrane is typically a gap of ~10 nm and covers an area with a radius of 200 nm (5). These dimensions are sufficiently small to result in restricted diffusion of soluble components, the diffusion of which is further restricted by the protrusion of protein domains, particularly RYR domains, into the dyadic space. The movement of Ca^{2+} in this space has not been observed experimentally, as the kinetics of movement and the small size of the dyad impose technical barriers that are difficult to overcome. Instead, a number of groups has used computational methods to predict dyadic free calcium [Ca^{2+}]$_{dyad}$, which range from ~10 μM to ~7 mM (5–9).

Many proteins resident in the dyadic region are controlled by both Ca^{2+} and site-specific phosphorylation (10). It has been long established that phosphorylation of DHPR increases Ca^{2+} current (I_{Ca}), probably by increasing the open probability (P_o) of the channel (11). Ca^{2+} also regulates RYR. Submicromolar Ca^{2+} is capable of activating RYR, but the maximal P_o is reached at ~100 μM, with higher (>5 mM) Ca^{2+} leading to inactivation of the channel (12,13). Although it is well established that both cAMP-dependent protein kinase (PKA) and calcium-calmodulin-dependent kinase II (CaMKII) phosphorylate RYR (14–16), the role of phosphorylation of RYR remains a contentious issue. It has been shown that RYR can be phosphorylated by both PKA and CaMKII in vitro at Ser-2809 (or Ser-2808, in humans) (14,15,17). Changes occurring upon in vitro phosphorylation at Ser-2809 are significant, including an increased P_o (15,17), the abrogation of the inhibitory effects of calmodulin (CaM) (15) and Mg^{2+} (18), an increased Ca^{2+} sensitivity of P_o (19), dissociation of regulatory factors (e.g., FKBP12.6), expression of subconductance states, and the expression of channel activity at diastolic [Ca^{2+}]$_{free}$ (17). Clinically, hyperphosphorylation of RYR at Ser-2808 has been described in situations such as heart failure, suggesting abnormal control of the phosphorylation status may contribute to abnormal Ca^{2+} handling (20), although more recent studies in vivo have noted no increase in Ser-2808

Submitted February 27, 2006, and accepted for publication March 27, 2006.

Address reprint requests to Dr. Peter P. Jones, Dept. of Physiology and Biophysics, University of Calgary, 3330 Hospital Dr. NW, Calgary, Alberta T2N 4N1, Canada. Tel.: 403-220-3055; Fax: 403-220-2211; E-mail: pjones@ucalgary.ca.

0006-3495/06/07/433/11 $2.00

doi: 10.1529/biophysj.106.083931

phosphorylation in failing canine, rat, or human hearts (21). Ser-2030 has also been described as a target for PKA phosphorylation, with a recent study suggesting that it is the major RYR phosphorylation target in response to β-adrenergic stimulation (21). To date no effect on Ca^{2+} handling has been reported relating to RYR Ser-2030 phosphorylation.

The RYR channels may play a more important role in β-adrenergic signaling as scaffold proteins, as they form a complex that localizes PKA and phosphatases 1 and 2A in the dyad (17). This is thought to ensure efficient local control of the phosphorylation status of RYR and other neighboring proteins.

A number of protein kinases have been reported to be affected by high [Ca^{2+}] because of the effect of Ca^{2+} on the level of MgATP. An increase in [Ca^{2+}] shifts the MgATP $\Leftrightarrow$ CaATP equilibrium toward CaATP, thus reducing MgATP. Additionally, specific ATP hydrolyzing proteins such as Juvenile Hormone Diol kinase (22) and the H^+,K^+-ATPase (23) will bind CaATP but not hydrolyze it efficiently. In these enzymes CaATP blocks the access of MgATP to the catalytic sites of the kinases and so is effectively a competitive inhibitor. Bhatnagar et al. (24) have reported that PKA will bind CaATP with a similar apparent affinity as MgATP but cannot hydrolyze CaATP to CaADP. These data suggest that PKA will be competitively inhibited by Ca^{2+} (through an increase in CaATP). If this occurs, it poses an interesting situation for the control of dyadic proteins by phosphorylation, where the normal extremes of $[Ca^{2+}]_{dyad}$ may affect kinase activity.

Here we show that PKA activity is inhibited by high [Ca^{2+}] as a result of an increase in [CaATP]. We have also developed a computer model of a ventricular myocyte incorporating the dyad that allows us to predict the extent to which PKA inhibition would occur in vivo.

METHODS

Materials

PKA was purchased from Upstate (Charlottesville, VA), PL919Y (synthetic peptide substrate, RSAIRRASTIEY-amide) was synthesized by Neosystem (Strasbourg, France), [γ-^{32}P]ATP was obtained from MP Biomedicals (Irvine, CA), and P81 paper was purchased from Whatman (Brentford, UK). All other chemicals were purchased from Sigma-Aldrich (Poole, UK).

Phosphorylation assays

Phosphorylation reactions were conducted at 37°C in 100 μl buffer containing 400 U (1 U is 1 pmol phosphate incorporation into PL919Y at 37°C per min) PKA, 0.1 mM PL919Y, and 50 mM histidine (pH 7.0), 5 or 25 mM $MgSO_4$, 6.25 mM NaF, 1 mM EGTA, and $CaCl_2$ to achieve $[Ca^{2+}]_{free}$ of 3 μM–10 mM (calculated using Bound and Determined (BAD) 4.42 (25)). After 2 min of equilibration the phosphorylation reaction was initiated by the addition of 0.1 mM [γ-^{32}P]ATP (0.1 μCi/nmol, final concentration to 10 μM). After 1 min of incubation the reaction was terminated by the addition of 100 μl 1% (v/v) H_3PO_4 to the sample and transferring 180 μl of sample to P81 paper. P81 paper was then washed 4× 5 min in 1% (v/v) H_3PO_4 before drying. Incorporated [γ-^{32}P] was determined by scintillation counting in Emulsifier-safe using a Packard TriCarb 1900TR scintillation counter, counting for 2 min per sample (both from Canberra-Packard Ltd., Pangbourne, UK).

Three-dimensional model of a sarcomere

The three-dimensional model of the half cardiac sarcomere is shown diagrammatically in Fig. 1. The sarcomere was cylindrical in shape (radius 500 nm; length 1000 nm). Ca^{2+} diffusion and regulatory processes were described by the following partial differential equation, which was solved using the implicit Euler's method of solution

$$\frac{\partial [Ca]}{\partial t} = \frac{D}{r}\left\{\frac{\partial}{\partial r}\left(r\frac{\partial [Ca]}{\partial r}\right) + \frac{\partial}{\partial \theta}\left(\frac{1}{r}\frac{\partial [Ca]}{\partial \theta}\right) + \frac{\partial}{\partial z}\left(r\frac{\partial [Ca]}{\partial z}\right)\right\} + F(r, \theta, z, [Ca], t), \quad (1)$$

where r, θ, and z are the radial, angular, and length dimensions in a cylindrical coordinate system, D is the diffusion coefficient, and $F(r,\theta,z,[Ca],t)$ is a function describing the position, concentration, and time-dependent Ca^{2+} regulatory processes and buffering included in the model. Similar equations were used to describe the diffusion of Mg^{2+} and the Ca^{2+} and Mg^{2+}-bound forms of ATP and ADP in the model. The modeled cell segment was divided into 50 radial elements (each one extending 10 nm in the radial direction), 50 length elements (10-nm long within the dyad, 20.6-nm long outside of the dyad), and 20 (18°) angular elements. The SR was represented by a disk located 10 nm from the plasma membrane with a radius of 200 nm, and a thickness of 20 nm in the z-direction (see Fig. 1). These dimensions are in keeping with those reported in the literature (5). At the start of the simulations, extracellular [Ca^{2+}] was assumed to be 1 mM, SR luminal [Ca^{2+}] was assumed to be 0.7 mM, and resting $[Ca^{2+}]_{free}$ was assumed to be 100 nM (26). Euler's method of solution of Eq. 1 requires that diffusion be computed into one element at each position beyond the boundaries of the model. This was achieved by setting all of the components in each element

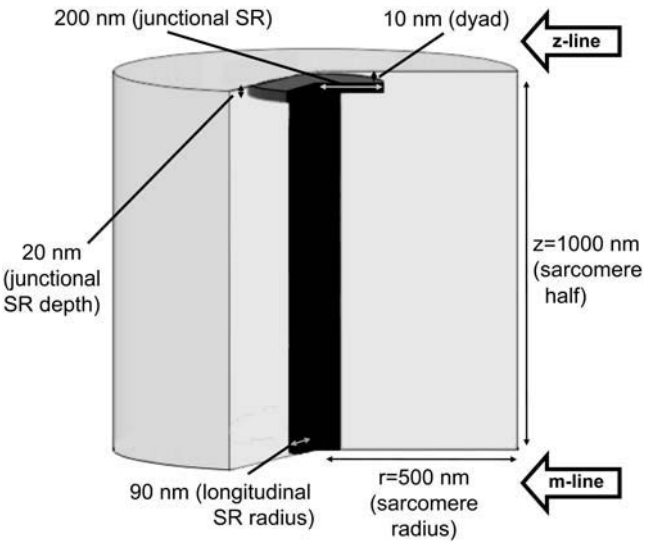

FIGURE 1 Cartoon of the computer model representing half of a sarcomere (Z-line to M-line). The position in the sarcomere is expressed in cylindrical coordinates (r,z,θ). The model is a cylinder with radius, r = 500 nm, length, z = 1000 nm. The junctional SR is modeled as an impermeable disk with radius, $r1$ = 200 nm, depth = 20 nm, situated 10 nm from the Z-line surface. Longitudinal SR is represented as a cylinder with radius = 90 nm and length = 970 nm. Free diffusion was allowed to occur throughout the longitudinal SR; however, SERCA uptake also occurred in this region. In r, the model is divided into 10-nm elements; in z the element size is 10 nm above and including the SR and 20.6 nm below, radially, the model is divided into 20 even segments. Calcium enters the model through the 20 radial segments at r = 1. Free [Ca^{2+}], CaATP, MgATP, CaADP, and MgATP are obtained for each element at 1-ms intervals.